Asian Journal of Chemistry; Vol. 33, No. 3 (2021), 658-664

ASIAN JOURNAL OF CHEMISTRY

https://doi.org/10.14233/ajchem.2021.23065

Characterization of Polymer Powders and Effects of Powder Reuse in Selective Laser Sintering

H. CHIRIRIWA

Department of Chemical Engineering, Vaal University of Technology, Private Bag X021, Vanderbijlpark, 1911 Andries Potgieter Blvd, South Africa

Corresponding author: E-mail: harrychiririwa@yahoo.com

Received: 11 November 2020; *Accepted*: 22 January 2021; *Published online*: 16 February 2021; AJC-20265

Selective laser sintering (SLS) had been recognized as production expertise (additive manufacturing). The complication restricting the use of SLS in additive manufacturing in an extensive range of industrial scope is the limited selection of usable polymers as it is only limited to polyamide 12. Other polymeric materials such as polypropylene and polyethylene are needed to establish pristine market avenues in industry. In selective laser sintering, the powder is reused in consecutive cycles of the route for the reason that it is sustainable and cost effective. Characterization procedures, including the many available techniques has been proposed to determine changes in chemical microstructures, morphology along with flowability. Subtle disimilarities linking virgin and used powder have been identified through characterization.

Keywords: Polymer powders, Selective laser sintering, Additive Manufacturing, 3D Printing.

INTRODUCTION

Laser sintering (LS) or selective laser sintering (SLS) is a layer producing technique, which utilizes material that is powdered, mainly thermoplastics and a CO_2 laser to fuse and discerningly heats the powder to form a layer which is complete [1-3]. This technique is found in the powder bed fusion category and allows manufacture of intricate and functional metal parts [4-6]. The strong point of the additive manufacturing (AM) methods as equated to other conventional production techniques such as injection moulding, is that more intricate and geometrically intricate parts can be manufactured without requirements of mould tools. These processes are especially equipped to produce low volumes of parts and in addition enable the production of compact miniature batch sizes with customized properties leading to reasonable costs [7,8].

Nylon polyamide (PA2200) is an extremely tough but flexible material in 3D printing and has high adhesion between layers [9,10]. Nylon polyamide (PA2200) has some disadvantages such as degradation after processing and its water absorption characteristic [11,12]. One of the major benefits of this material is its high reprocessability to a value of 50% by weight for a new common laser sintering process [13]. The success of this powder then is not only because of its good properties in terms of flow and processability but also due to its cost that it is made competitive through its high recycling performance [14,15]. According to Kruth *et al*. [16] polyamide powder can be recycled for a certain number of runs, until the flowability becomes detrimental for the spreading of powder within a laser sintering system and the melt viscosity increases up to a point that causes deleterious surface finishing effects in the parts, known as "orange peeling".

The aim of this research is to assess the useability of polyolefins specifically polyamide (PA 2200) in the selective laser sintering (SLS) applications and poly(methyl methacrylate) (PMMA). The investigation is centered on a theoretical review as well as some experimental investigations to study polyamide (PA2200) and the deterioration of the powder properties during laser sintering and suggest a system of methods for systematic polymer powder recycling.

EXPERIMENTAL

In selective laser melting polyamide 12 (PA2200) powder is used commercially. An unmodified PA12 laser melting powder type PA2200 form the supplier EOS GmbH, Germany was

used [17]. The categories 'used' and 'virgin' will be used to mention the state of metal powders [18]. The virgin state applies to powder as obtained from supplier and used refers to the same powder batch that has been employed in the operation for more than one build cycle. Nylon polyamide PA2200 is white in colour, has a melting temperature 176 ºC [19] and an onset crystallization temperature of 150-152 ºC. Accessible in a distinct number of composite materials optimized for laser sintering, PA2200 is one of the most well accepted materials for laser sintering. It powder exhibits good chemical resistance, high strength and stiffness, biocompatibility and offers the potential for surface finishing [20].

Infrared spectroscopy: Fourier transform infrared spectroscopy (Thermoscientific Nicket IS10) was used to characterize the PA2200 and PMMA.

X-ray diffraction: X-ray diffraction (XRD) patterns were taken using a Philip X Pert X ray diffractometer (anode 45 kV, filament current 40 mA) with a nickel filtered CuKα (λ = 0.1545 nm) radiation with scan speed of 1º/min in this work. Scans were recorded from 0 to 35º on fine attenuated sheet samples prepared *via* compression moulding.

Particle size distribution: The PA2200 and PMMA were investigated using Olympus BX 41 optical microscope. Particles and size distribution was measured *via* optical imaging. According to this a small amount of powder is distributed on a glass plate and afterwards with a microscope an image of each particle is taken. All experiments were carried out in duplicates and resolved in triplicates to corroborate the accuracy of the procedure.

Polarized optical microscopy: Spherulites in PA2200 and PMMA were examined using a cross polarized Leica DMRX optical microscope. Specimens were melted at 215 ºC for 5 min and pressed between microscope glass cover slides to produce a thin layer before cooling to ambient temperature.

Melt-flow rate: Melt flow rate is a measurement of a melted thermoplastic and how easily it flows. This is expressed as g/10 min in SI units. Alternately, the volume flow rate (VFR) (cm^3/10 min) can also be used. A small thermoplastic sample (granule, flake, powder) is heated to a viscous state in a heated barrel and extruded through a capillary die. A piston loaded with dead weights forces the melted plastic material through a capillary die. After enough sample material has been extruded, it is removed and weighed [21]. Fig. 1 shows a melt-flow index machine and corresponding diagram of internal components.

The die size, barrel temperature and piston force are set per standards for each tested material. In order to lower the noise and disparity in the MFR measurement, three quantifications from each same sample were taken and standards determined.

Particle size distribution: The particle size distribution (PSD) test gives the size distribution of the single units, particles or grains, constituting a bulk material. The scope of this technique has been to evaluate the particle size distribution of established laser sintering materials and new potential powders. Most of the tests were evaluated by employing a Saturn DigiSizer. The instrument gives the distribution size of particles in a sample and detected by light scattering. The sample is suspended in a specified solution and hit by a laser source, hence creating a diffraction pattern specific to size of the particles involved. A solution of 0.5% sodium hexametaphosphate is used.

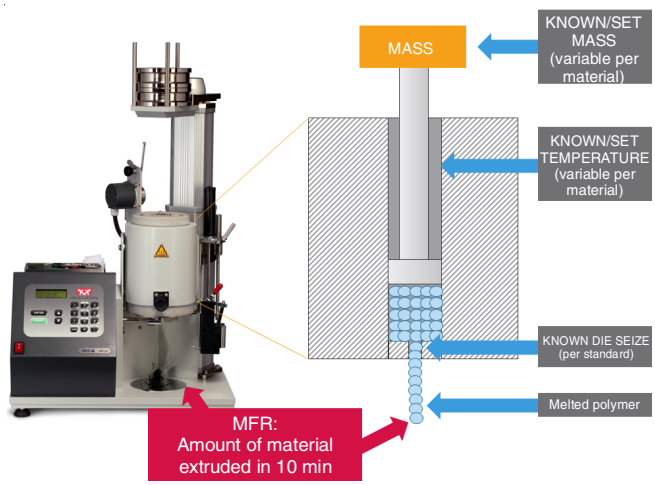

Fig. 1. Melt-flow rate index machine and diagram of internal components

Three measurements were performed on the individual material and average responses of the three repeats were recorded. Although this test assumes that the particles are spherical or nearly spherical, it is widely used in the laser sintering community and therefore utilized here.

RESULTS AND DISCUSSION

Infrared spectroscopy: The FTIR spectra in Fig. 2 shows that there is not much change of chemical structure on the virgin PA 2200 and damaged PA 2200 powders. In Fig. 2, the predictable adsorption peak at 3303 cm^{-1} is for NH vibration and bands close to 2938 and 2864 cm^{-1} represent CH_2 vibration. The amide absorption (C=O) at 1636 cm^{-1} and the amide absorption (N-H) at 1539 cm^{-1} can be also seen.

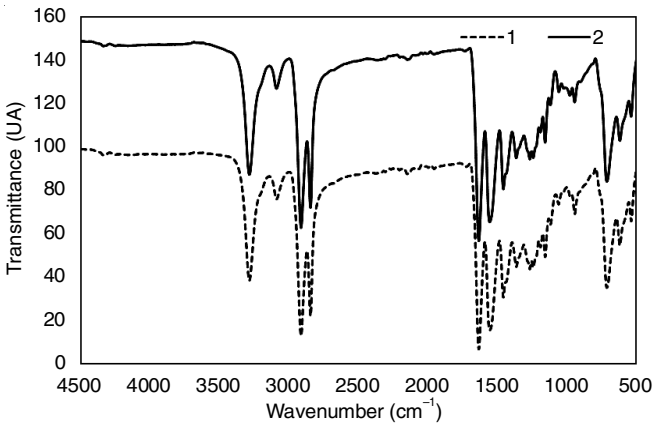

Fig. 2. FTIR spectra of (1) PA2200 virgin, (2) PA200 used

The spectrum of virgin PMAA is also the same as that of damaged PMMA as shown in Fig. 3. Absorption bands were seen at 2995-2953 cm^{-1} (-CH_3 and -CH_2 stretching, respectively), 1433 cm^{-1} (-CH_2; bending vibration), 1065 cm^{-1} (C-O; bond stretching), 1386-749 cm^{-1} (α-methyl group vibrations), as well as PMMA absorption bands at 1194-1146 cm^{-1} and shifting of

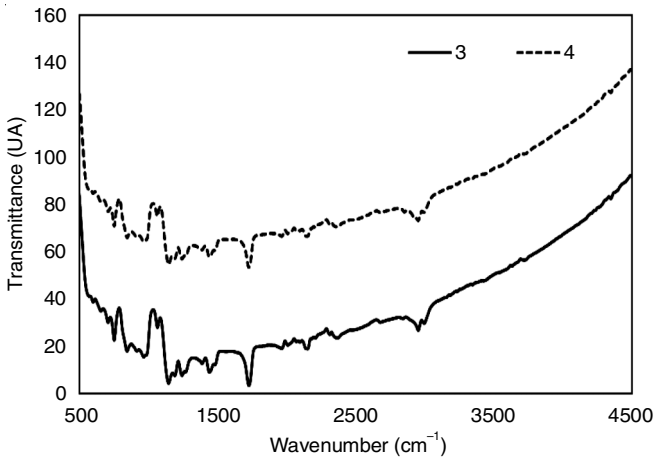

Fig. 3. FTIR spectra of (3) PMMA virgin, (4) PMMA damaged

oxygen bonded to CH_3 (ether group O-CH_3). Intense absorption bands at 1725 cm^{-1}, associated to stretching of carbonyl group (C=O), are also observed in the spectra, which is found to conform with the prior reported observations [22-24]. Numerous intense absorption bands are observed under 1510 cm^{-1} and the region has strong absorption features owing to varying (C-H) deformation modes of methyl subunits in the range ~1510 to 1350 cm^{-1}. The (C-C-O) stretching vibrations from methyl of the carbonyl group is seen in the range 1265 and 1155 cm^{-1} whereas (C-O-C) vibrations are located in the range 1195 to 1155 cm^{-1}. The absorption features under 1005 cm^{-1} have been allocated to C-H rocking modes together with C-C skeletal modes [25].

X-ray diffraction: As stated by Khanna & Kuhn [26], PA2200 may have two distinct crystallographic forms, γ-pseudo-hexagonal and α-monoclinic. Hydrogen bonds form between antiparallel chains in α-form whilst in γ-form hydrogen bonds are found in parallel chains causing the molecular chains to twist in a zig-zag manner. The crystal density, heat of fusion of γ-form where interactivity between chains are weaker and less in the α-form as a result of this phenomenon. The α-form is observed in the XRD pattern exhibiting a diffraction peak at 2θ round about 24.1°. Semi crystalline γ-form observed in Fig. 4 with a peak between 21.1 and 22.1°.

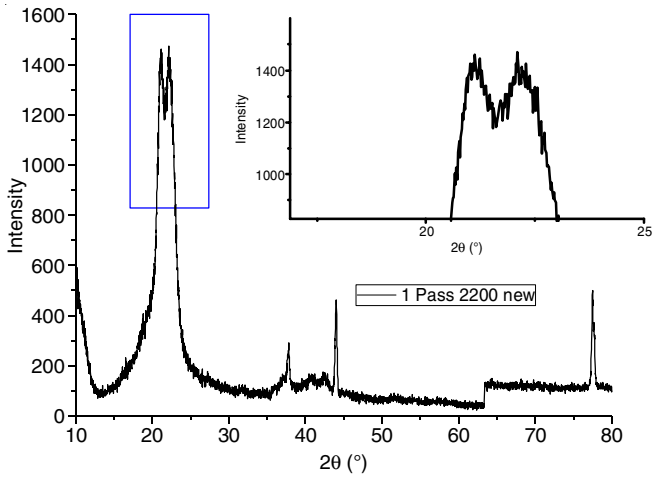

Fig. 4. XRD pattern of virgin PA2200

The XRD pattern of damaged PA2200 also exhibits similar characteristics as that observed in the virgin PA2200 powder as shown in Fig. 5. poly(methyl methacrylate) (PMMA) is an amorphous polymer which is well known. The shape of the initial most intense peak at 2θ values of 13° and 23.7° and *d* spacing at about 3.745, 3.742 reflects the ordered packing of polymer chains while the second peak denotes the ordering inside the main chains with their intensity decreasing methodically as shown in Fig. 6. This accounts for the homogenous identity of PMMA thin films and identical results have been documented [27]. Pure PMMA shows the principal and broad peak with a maximum at 2θ 13.2° along with broad but low intensity peak at 31° and 35°. The broad peaks demonstrate the amorphous nature of the polymer as described in literature [28,29]. The peaks appear at 2θ: 13.20°, 15.95°, 31.04°, 35.00°, corresponding to the diffraction pattern of (111), (002), (112) and (211) plains, respectively. The observed broad humps in the XRD spectrum indicate the existence of crystallites of very low dimensions. The absence of any prominent peaks in the PMMA thin films indicates its amorphous nature [30]. Similar corresponding peaks are also observed in the recycled PMMA as shown in Fig. 7.

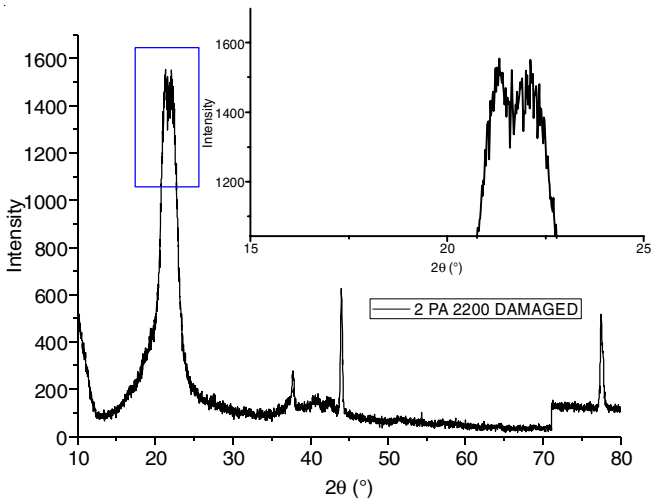

Fig. 5. XRD pattern of damaged PA2200

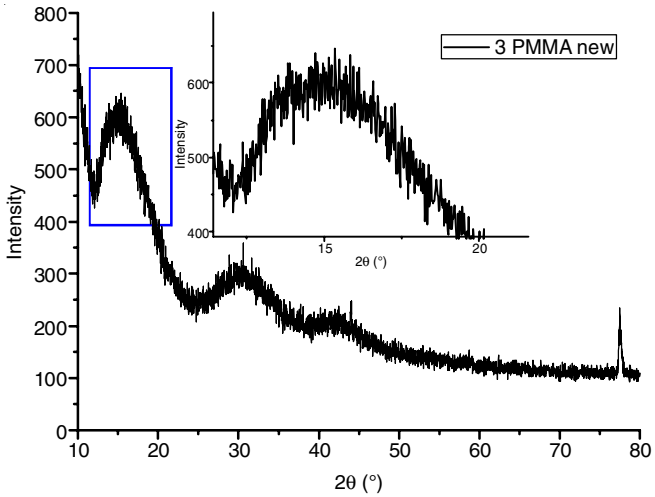

Fig. 6. XRD pattern of virgin PMMA

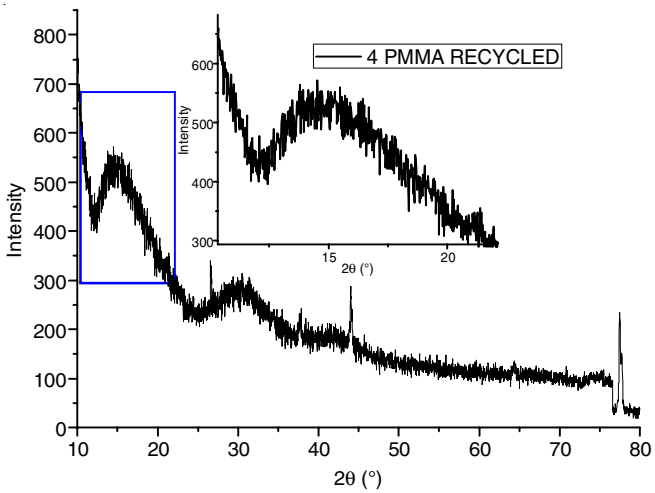

Fig. 7. XRD pattern of recycled PMMA

Particle size distribution: Powders must have a certain particle size distribution (PSD) and the distribution is positively around 20 µm and 80 µm. Fig. 8 showed that the virgin PMMA appears to be of finer sizes and the recycled PMMA exhibits the most of the coarse powder or granular particles. With respect to the cumulative distribution (Fig. 8), no significant difference is visible between the virgin and aged powders. It can be concluded from this result that systematic aging of PA2200 or PMMA powders neither led to a change of density nor the cumulative distribution.

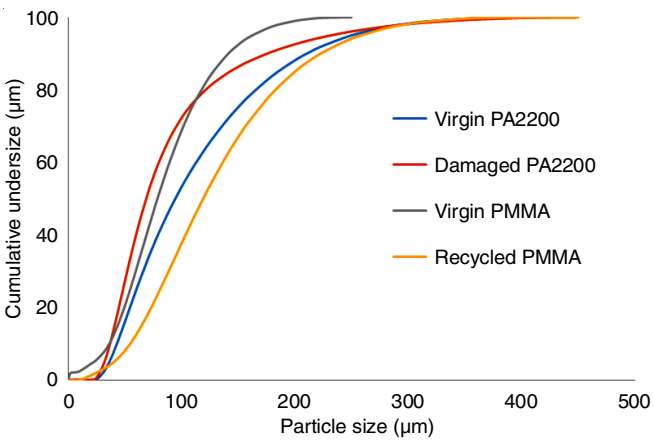

Fig. 8. Particle size distribution for PA2200 virgin/recycled and PMMA virgin/recycled

Polarized optical microscopy: The particles look circular or slightly elongated, round with smooth but cracked surface in both materials. As PA2200 represents a well-established laser sintering material. Most of the particles confirmed to be round and nearly spherical as observed in Figs. 9 and 10. This result indicates that there is not much differentiation between the contrasting particle sizes even when the powder was repeatedly used.

From Figs. 11 and 12, it is very clear that for both virgin and new PMMA polymer powders the light is being reflected back and hence no clear images can be observed. This may be attributed to cohesive forces between the powder particles and there might also be static interactions. The recycled PMMA does not have any flowing properties like the virgin PMMA and seems to clump together in a distinct mass. It is a highly electrostatic powder and the electrostatic charges generated on polymer powders during mixing may lead to electrostatic problems due to the poor conductivity of these powders. To eliminate the charge on the powder, several methods such as ionization, humidification and addition of an antistatic agent have been practiced in industrial processes [31].

Electrostatic charging is a complex prodidy when handling mixtures of powders that are polydisperse particles as a result of bipolar charging where small particles become charged opposite to their counterparts, which are larger. Bipolar charging leads to drawbacks such as segregation, agglomeration and critical adhesion to contact surfaces or walls. In order to characterise electrostatic properties of powders, it is prudent to measure not only the polarity but also the charges on a powder [32]. Tiny particles carry negative charges when exposed to coarse counterparts of similar material. They however carry a positive charge from charge transfer of conductive contact walls.

Electrostatic charge build-up is significantly enhanced for aged polymer powder material, likely contributing to altered

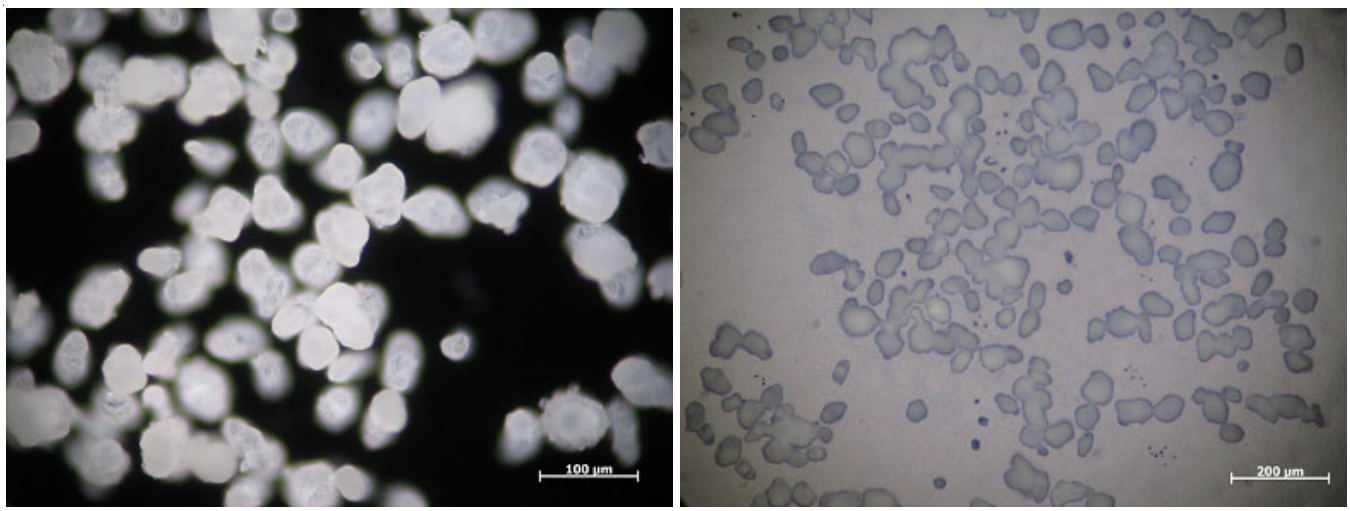

Fig. 9. Optical microscope images of virgin PA2200 at different magnifications

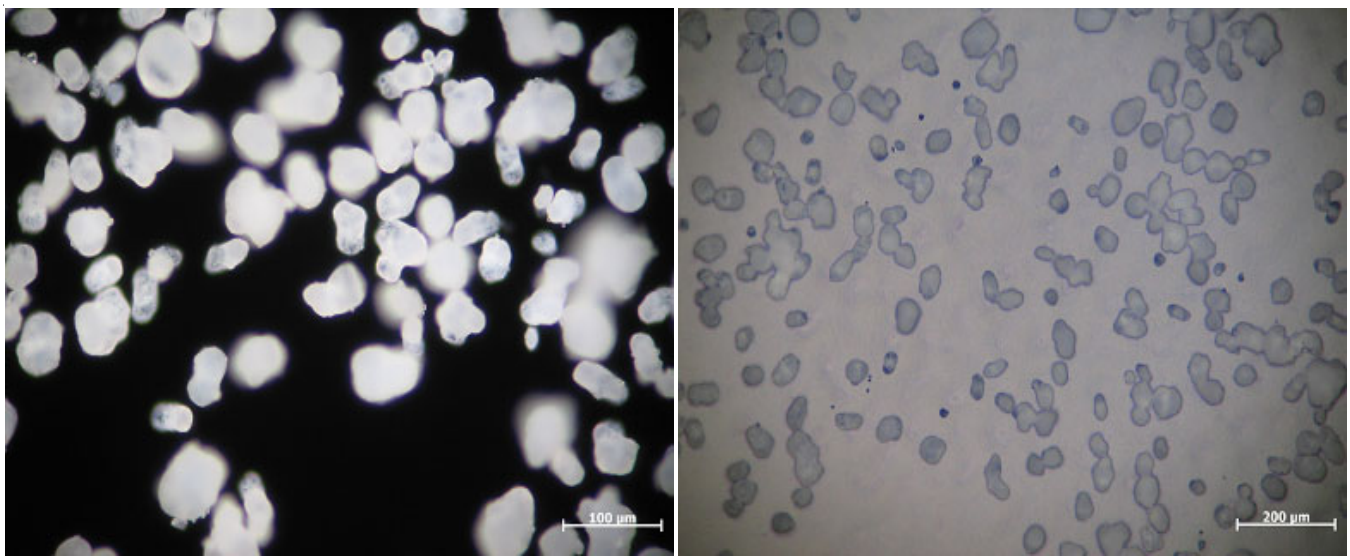

Fig. 10. Optical microscope images of "used" PA2200 at different magnifications

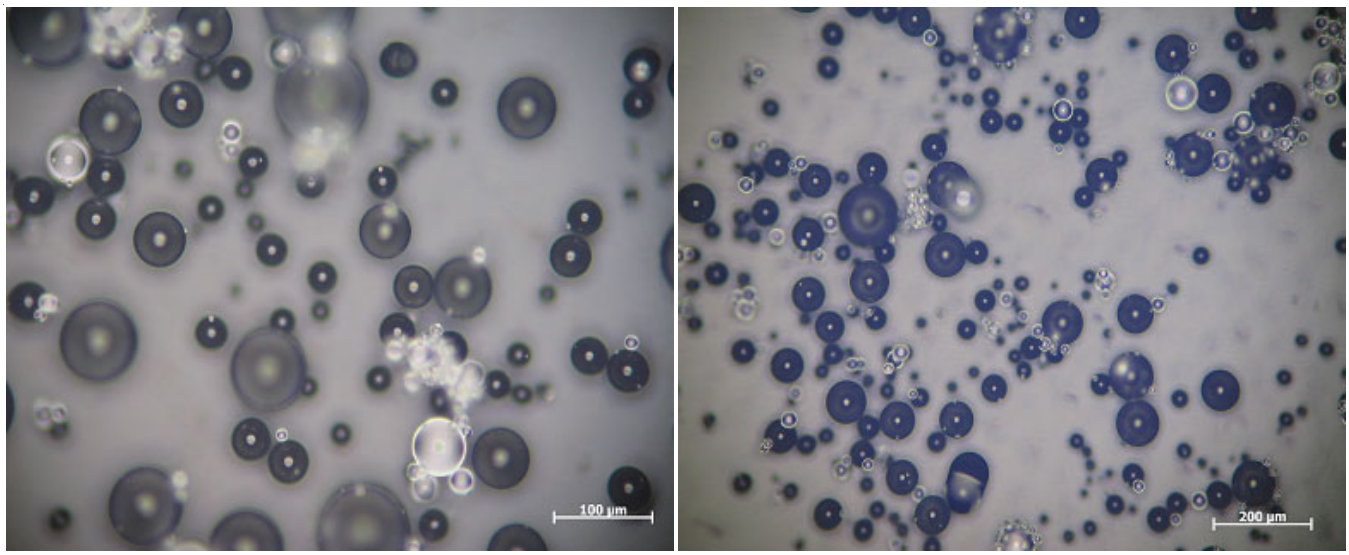

Fig. 11. Optical microscope images of virgin PMMA at different magnifications

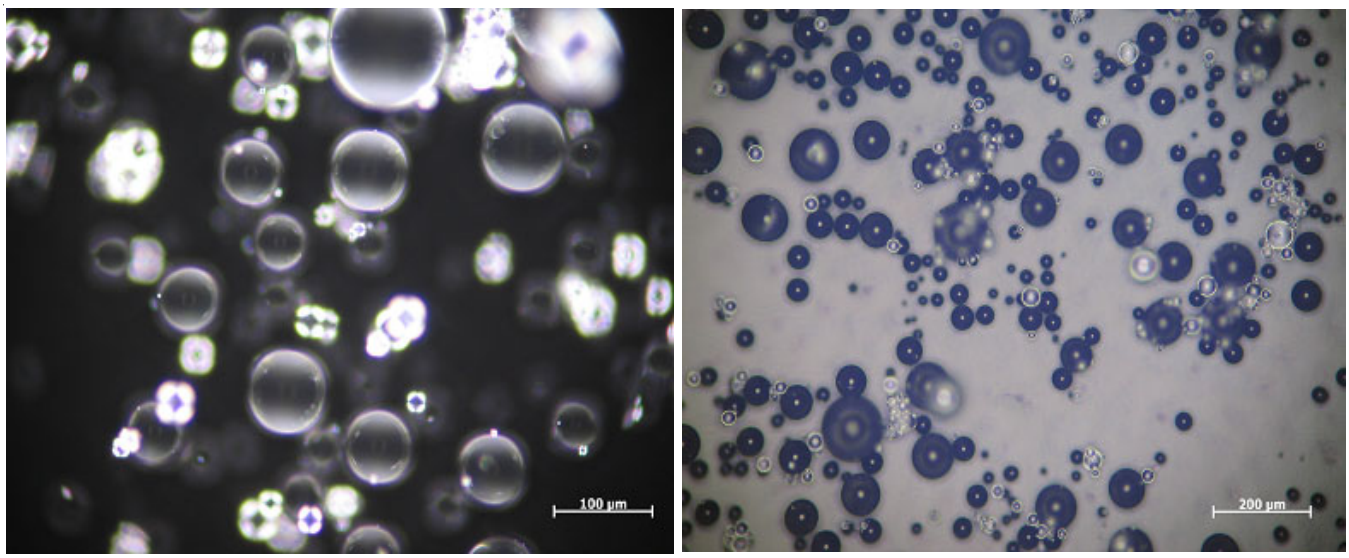

Fig. 12. Optical microscope images of "used" PMMA at different magnifications

performance in SLS processing [33]. Due to the elevated temperatures during processing, polymer powders can exhibit altered properties even though they are not used for part generation [34,35]. Especially polyamides suffer from high temperatures because of solid-state post-condensation, resulting in a prolonged molecular chain length.

Melt-flow rate: A melt flow rate (MFR) test is conducted to establish quality of the powder. A high MFR means that the material is likely to be virgin material and will have better thermal and processing properties. From Fig. 13, a melt flow rate of 36.76 g/10 min was observed for the virgin PA2200 with the damaged powder having a rate of 7.47 g/10 min. Low resistance to flow in the virgin PA2200 is a result of low entanglement with a short molecular chain. "Recycled PA2200" morphology has longer molecular chains and this means melt viscosity and higher molecular weight.

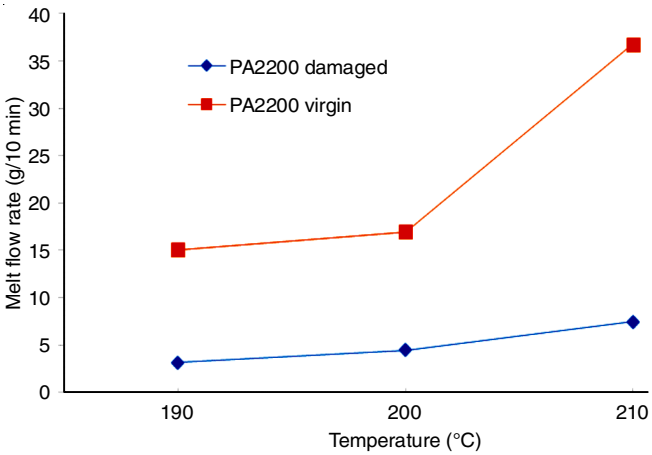

Fig. 13. Comparison of virgin to used PA2200

The chemical structure of any polymer determines its flowability. Polymer chains having non-complex geometry and are relatively of short length, slide past one another easily with little or no flow resistance. By disparity, long chains of high molecular weight and complex structure produce viscocity and greater flow resistance [36-38].

Fig. 14 shows that by adding the higher amount of better quality PA2200 increases gradually the MFR value. This means that the powder quality and melt viscosity are correlated. This could be due to the less deteriorated PA2200 powder having a lower entanglement with a shorter molecule chain, which initiates a higher MF value and thus low resistance to flow. This could produce a better powder melting and fusion during the sintering process. The melt viscosity improves when the less deteriorated powder was blended.

The MFR was chosen as a benchmark because the flow attributes of a molten polymer are very responsive to changes in the basic polymer structure and its molecular weight [39,40]. The fundamental polymer property that is measured in this test is the molten plastic flow at a particular shear stress that is related to the applied load and temperature. The MFR test accords a comparatively rapid and economical measuring method of the rate of degradation of PA2200 powder during the laser sintering process.

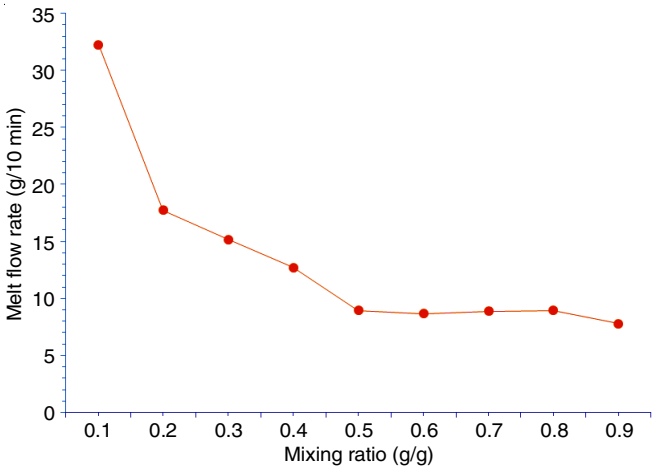

Fig. 14. Comparison of damaged to virgin PA2200 at optimum temperature

Powder quality and melt viscosity are correlated. This could be due to the less deteriorated PA2200 powder having shorter molecular chains with lower entanglement leading to a higher MFR value and thus a low resistance to flow. This could produce a better powder melting and fusion during the sintering process, which results in a good surface finish. Melt flow index (MFI) indicates how viscous a polymeric molten material is. The smaller the MFI value is, the more viscous the polymer [41].

Conclusion

It was validated that the melt flow rate (MFR) index is a subtle and delicate measure of changes in properties of the powder and accords a relatively quick and cheap method of calculating the rate of degradation of polymer powder during the laser sintering process.

ACKNOWLEDGEMENTS

The author is grateful for an award of a Fellowship from Centre for Rapid Prototyping and Manufacturing (CRPM), Central University of Technology, Republic of South Africa.

CONFLICT OF INTEREST

The authors declare that there is no conflict of interests regarding the publication of this article.

REFERENCES

1. M. Touri, F. Kabirian, M. Saadati, S. Ramakrishna and M. Mozafari, *Adv. Eng. Mater.*, **21**, 1800511 (2019); https://doi.org/10.1002/adem.201800511
2. S. Berretta, K.E. Evans and O.R. Ghita, *Mater. Des.*, **105**, 301 (2016); https://doi.org/10.1016/j.matdes.2016.04.097
3. C.A. Chatham, T.E. Long, C.B. Williams, *Progr. Polym. Sci.*, **93**, 68 (2019); https://doi.org/10.1016/j.progpolymsci.2019.03.003
4. L. Cordova, M. Campos and T. Tinga, *JOM*, **71**, 1062 (2019); https://doi.org/10.1007/s11837-018-3305-2
5. W.S.W. Harun, M.S.I.N. Kamariah, N. Muhamad, S.A.C. Ghani, F. Ahmad and Z. Mohamed, *Powder Technol.*, **327**, 128 (2018); https://doi.org/10.1016/j.powtec.2017.12.058
6. D. Herzog, V. Seyda, E. Wycisk and C. Emmelmann, *Acta Mater.*, **117**, 371 (2016); https://doi.org/10.1016/j.actamat.2016.07.019

7. N. Hopkinson, R.J.M. Hague and P.M. Dickens, Rapid Manufacturing: An Industrial Revolution for the Digital Age, John Wiley & Sons, Ltd.: Chichester, England, pp 285 (2006).
8. R.D. Goodridge, C.J. Tuck and R.J.M. Hague, *Prog. Mater. Sci.*, **57**, 229 (2012); https://doi.org/10.1016/j.pmatsci.2011.04.001
9. N. Lammens, M. Kersemans, I. De Baere and W. Van Paepegem, *Polymer Testing*, **57**, 149 (2017); https://doi.org/10.1016/j.polymertesting.2016.11.032
10. J.R.C. Dizon, A.H. Espera Jr., Q. Chen and R.C. Advincula, *Addit. Manufact.*, **20**, 44 (2018); https://doi.org/10.1016/j.addma.2017.12.002
11. C.M. González-Henríquez, M.A. Sarabia-Vallejos and J. Rodriguez-Hernandez, *Progress Polym. Sci.*, **94**, 57 (2019); https://doi.org/10.1016/j.progpolymsci.2019.03.001
12. R. Goodridge, S. Ziegelmeier, Woodhead Publishing Series in Electronic and Optical Materials, pp 181-204 (2017).
13. EOS, EOSINT P 100 manual.
14. A.F.A. Becker, Ph.D. Thesis, Characterization and Prediction of SLS Processability of Polymer Powders with respect to Powder Flow and Part Warpage, pp. 21 (2016).
15. L. Verbelen, S. Dadbakhsh, M. Van den Eynde, J.P. Kruth, B. Goderis and P. Van Puyvelde, *Eur. Polym. J.*, **75**, 163 (2016); https://doi.org/10.1016/j.eurpolymj.2015.12.014
16. J.P. Kruth, X. Wang, T. Laoui and L. Froyen, *Rapid Prototyping J.*, **23**, 357 (2003); https://doi.org/10.1108/01445150310698652
17. EOS. http://www.eos.info/en/home.html
18. BS ISO/ASTM 52900:2015, Standard Terminology for Additive Manufacturing-General Principles-Terminology (BSI Standards Limited: London (2016).
19. EOS. PA 2200 material datasheet.
20. A. Mahmud, Ph.D. Thesis, Cardiff University, Cardiff, United Kingdom (2009).
21. E. Mangano, Understanding Melt Flow Testing and Its Importance (2014).
22. Ismayil, V. Ravindrachary, R.F. Bhajantri, S.D. Praveena, B. Poojary, D. Dutta and P.K. Pujari, *Polym. Degrad. Stab.*, **95**, 1083 (2010); https://doi.org/10.1016/j.polymdegradstab.2010.02.031
23. C.P. Ennis and R.I. Kaiser, *Phys. Chem. Chem. Phys.*, **12**, 14902 (2010); https://doi.org/10.1039/c0cp01130d
24. P. Tiwari, A.K. Srivastava, B.Q. Khattak, S. Verma, A. Upadhyay, A.K. Sinha, T. Ganguli, G.S. Lodha and S.K. Deb, *Measurement*, **51**, 1 (2014); https://doi.org/10.1016/j.measurement.2014.01.017
25. C.P. Ennis and R.I. Kaiser, *Phys. Chem. Chem. Phys.*, **12**, 14884 (2010); https://doi.org/10.1039/c0cp00493f
26. Y.P. Khanna and W.P. Kuhn, *J. Polym. Sci.*, **35**, 2219 (1997); https://doi.org/10.1002/(SICI)1099-0488(199710)35:14<2219::AID-POLB3>3.0.CO;2-R
27. R. Hussain and D. Mohammad, *Turk. J. Chem.*, **28**, 725 (2004).
28. N.J. Hameed Al-Mashhadan and S. Mohamad, *Eng. Tech. J.*, **29**, 20 (2011).
29. Q. Xia, X.J. Zhao, S.J. Chen, W.Z. Ma, J. Zhang and X.L. Wang, *Express Polym. Lett.*, **4**, 284 (2010); https://doi.org/10.3144/expresspolymlett.2010.36
30. A. Ahmad, M.Y.A. Rahman and H. Hamzah, *Open Mater. Sci. J.*, **5**, 170 (2011); https://doi.org/10.2174/1874088X01105010170
31. K.S. Choi, M. Omar, X. Bi and J.R. Grace, *J. Loss Preven. Process Ind.*, **23**, 594 (2010); https://doi.org/10.1016/j.jlp.2010.05.007
32. L. Zhang, X. Bi and J.R. Grace, *Procedia Eng.*, **102**, 295 (2015); https://doi.org/10.1016/j.proeng.2015.01.146
33. N. Hesse, M. Dechet, J. Bonilla, C. Lübbert, S. Roth, A. Bück, J. Schmidt and W. Peukert, *Polymers*, **11**, 609 (2019); https://doi.org/10.3390/polym11040609
34. K. Dotchev and W. Yusoff, *Rapid Prototyping J.*, **15**, 192 (2009); https://doi.org/10.1108/13552540910960299
35. C. Mielicki, B. Gronhoff and J. Wortberg, In Proceedings of the PPS-29: The 29th International Conference of the Polymer Processing Society—Conference Papers, Nuremberg, Germany, 15–19 July 2013; American Institute of Physics: College Park, MD, USA, pp. 728–731 (2014).
36. H.A. Barnes, J.F. Hutton and K.W. Walters, An Introduction to Rheology, Elsevier (1998).
37. R. Martin, A. Crispin and D. Angela, Multi-Rate and Extensional Flow Measurements using the Melt Flow Rate Instrument: Measurement Good Practice Guide, National Physical Laboratory (2001).
38. J. Martin, Materials for Engineering, Woodhead Publishing in Materials, edn 3, pp l59-184 (2006).
39. T.J. Gornet, CAD/CAM Publishing, pp 1-3 (2002).
40. T.J. Gornet, Proceedings of Solid Freeform Fabrication, Austin, Texas, pp 546-553 (2002).
41. D.T. Pham, K.D. Dotchev and W.A.Y. Yusoff, *Proc. Inst. Mech. Eng., C J. Mech. Eng. Sci.*, **222**, 2163 (2008); https://doi.org/10.1243/09544062JMES839